GUANGXI NORMAL UNIVERSITY

中国物理学会高能物理分会第十二届全国会员代表大会暨学术年会

# Study on the Deconfining Phase Transition under Real Rotation with the Matrix model

Du Qianqian(杜倩倩)

2026.07.15

## Outline：

- Background and Motivations
- Matrix model under real rotation
- Deconfining phase transition under real rotation
- Summary and Outlooks

# Background and Motivations

Hannah Petersen, Nature volume 548, pages34–35 (2017).

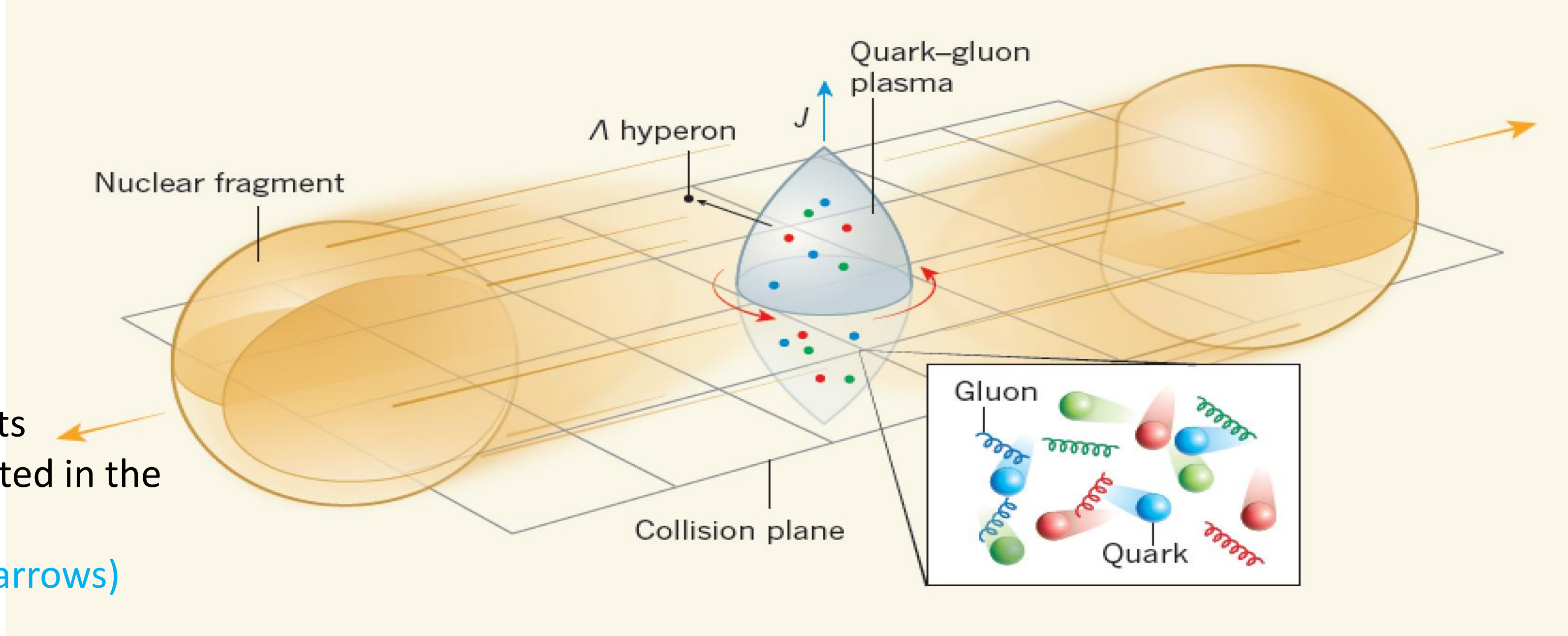


Nuclear fragments continue unaffected in the plane of the collision(orange arrows)

Fig. 1 Measuring the rotation of the quark–gluon plasma

1) QGP rapidly rotates, with an angular momentum, perpendicular to the plane of the collision.

2) The vorticity of QGP can be determined by using the polarization of Λ hyperons, due to its self-analysis, on experiment.

In experiment RHIC-STAR: $\boxed{\Omega \simeq (9 \pm 1) \times 10^{21} \mathrm{s}^{-1} \sim 6 \mathrm{MeV}}$ L. Adamczyk et al. (The STAR Collaboration), Nature 548, 62–65 (2017).

Hydrodynamic simulations: $\boxed{\Omega \sim 0.1 - 0.2 \mathrm{fm}^{-1} \sim 20 - 40 \mathrm{MeV}}$ Yin Jiang, Zi-Wei Lin, and Jinfeng Liao, Physical Review C 94, 044910 (2016), (AMPT model).

# Background and Motivations

Rotation affect ⟹ Chiral vortical effect | Polarization of particles | QCD phase transition

G. Y. Prokhorov, O. V. Teryaev, and V. I. Zakharov, J. High Energy Phys. 02 (2019) 146.

O. V. Teryaev and V. I. Zakharov, Phys. Rev. D 96, 096023 (2017).

1) Chiral phase transition

Rotation suppresses the chiral critical temperature.

Lattice QCD, NJL model, Holography, HRG model, Analytically tractable model in compact QED···

Hao-Lei Chen, Kenji Fukushima, Xu-Guang Huang, and Kazuya Mameda, Phys. Rev. D 93, 104052 (2016);
Yin Jiang and Jinfeng Liao, Phys. Rev. Lett. 117, 192302 (2016);
M. N. Chernodub and Shinya Gongyo, J. High Energy Phys. 01 (2017) 136; Phys. Rev. D 95, 096006 (2017);
Xinyang Wang, Minghua Wei, Zhibin Li, and Mei Huang, Phys. Rev. D 99, 016018 (2019);
Zheng Zhang, Chao Shi, Xiao-Tao He, Xiaofeng Luo, and Hong-Shi Zong, Phys. Rev. D 102, 114023 (2020);
N. Sadooghi, S. M. A. Tabatabaee Mehr, and F. Taghinavaz, Phys. Rev. D 104, 116022 (2021).

Explanation: Y. Jiang and J. Liao, Phys. Rev. Lett. 117, 192302 (2016).

The rotation tends to align the spins of quarks and antiquarks along the rotation axis, thus suppressing the scalar pairing and, therefore, lowering the scalar fermionic condensate.

## Background and Motivations

2) The deconfining phase transition

Lattice QCD by using Monte Carlo simulations

a) The deconfining temperature $T_c$ increases quadratically with $\Omega$;

Polyakov loop $\ell$ decreases with $\Omega$ in the deconfining phase.

V. V. Braguta, A. Yu. Kotov, D. D. Kuznedelev, and A. A. Roenko, JETP Lett. 112, 6–12(2020); Phys. Rev. D 103, 094515 (2021).

b) Rotated gluon plasma becomes spatially inhomogeneous ;

Local $T_c$ at rotation axis does not depend on $\Omega$ within a few percent accuracy;

$T_c$ increases with the distance from the rotation axis, violates the Tolman-Ehrenfest law;

$T_c$ increases quadratically with radial distance in the intermediate region;

$\ell$ decreases as radial distance increases.

V. V. Braguta, M. N. Chernodub, A. A. Roenko, Phys. Lett. B 855 (2024) 138783.

Lattice QCD by using strong coupling expansion method

$T_c$ decreases quadratically with $\Omega$.

Sheng Wang, Jun-Xia Che, Defu Hou, Hai-Cang Ren, e-Print: 2505.15487 [hep-ph].

## Background and Motivations

Holography QCD

$T_c$ increases with $\Omega$ ; Jun-Xia Chen, Sheng Wang, Defu Hou, Hai-Cang Ren, Phys. Rev. D 111 (2025) 2, 026020; Yidian Chen, Xun Chen, Danning Li, Mei Huang, Phys. Rev. D 111 (2025) 4, 046006.

$T_c$ decreases with $\Omega$. Xun Chen, Lin Zhang, Danning Li, Defu Hou, and Mei Huang, J. High Energy Phys. 07 (2021) 132; Jia-Hao Wang and Sheng-Qin Feng, Phys. Rev. D 109 (2024) 6, 066019.

Hadron resonance gas model

$T_c$ decreases with $\Omega$. Y. Fujimoto, K. Fukushima, and Y. Hidaka, Phys. Lett. B 816, 136184 (2021).

Analytically tractable model in compact QED

$T_c$ decreases with $\Omega$ and radial distance.

M. N. Chernodub, Phys. Rev. D 103, 054027 (2021).

Bag model

For static bag constant $B_0$, $T_c$ decreases with $\Omega$ ;

For $B(\Omega)$, $T_c$ increases with $\Omega$.

Kazuya Mameda, Keiya Takizawa, Phys.Lett.B 847 (2023) 138317.

Caloron model

Yin Jiang, Phys. Lett. B 853 (2024) 138655; Phys. Rev. D 110, 054047 (2024).

For SU(2), static coupling constant $g$, $T_c$ decreases with $\Omega$ ; $T_c$ increases with radial distance.

Along the rotation axis, for $g(\Omega)$, non-monotonic behavior, $T_c$ increases with small $\Omega$.

Perturbative method

Shi Chen, Kenji Fukushima, Yusuke Shimada, Phys. Rev. Lett. 129 (2022) 24, 242002; Phys. Lett. B 859 (2024) 139107.

At sufficiently large imaginary $\Omega_I$ , the system goes through a phase transition perturbatively.

At the perturbative level, no phase transition occurs along the rotation axis for any $\Omega$.

*The effect of the rotation on the deconfinement phase transition temperature is still controversial.*

# Matrix model under real rotation

## 1) The original matrix model (MMO)

The first two terms in high $T$ expansion of the 1-loop effective potential with effective mass $M$ and assuming $M \ll T$ by using **Background field effective theory (BF eff.)**

- Perturbation ($T^4$)
- **Non-perturbation($M^2T^2$)**

P. N. Meisinger, T. R. Miller, M. C. Ogilvie, Phys. Rev. D 65 (2002) 034009.

It can well describe the physical behavior of QGP near the deconfinement phase transition point.

## 2) The background field

A. T. Bhattacharya, A. Gocksch, C. P. Korthals Altes and R. D. Pisarski, Phys. Rev. Lett. 66, 998 (1991).

The **classical background field** is described by the diagonal matrix of the color space: $(A_0^{\text{cl}})_{ab} = \frac{2\pi T}{g} \mathrm{q}^a \delta_{ab}$,

where: $(\mathrm{q}^a - \mathrm{q}^b) \equiv \mathrm{q}^{ab}$ and $\sum_{a=1}^{N} \mathrm{q}^a = 0$, $a, b = 1, \cdots N$.

**Polyakov loop**:

$$\ell = \frac{1}{N} \mathrm{Tr}\, \mathcal{P} \exp\left(ig \int_0^\beta A_0^{\text{cl}}\, d\tau\right).$$

| Phase | Temperature | $\ell$ from LQCD | Method |
|---|---|---|---|
| hadronic | $T < T_d$ | $\ell = 0$ | eff. theory (HRG) |
| QGP | $T > \sim 3T_d$ | $\ell \approx 1$ | (HTL) pert. theory |
| "semi"-QGP | $T_d < T < \sim 3T_d$ | $0 < \ell < 1$ | **BF eff.** theory |

$T_d$ is deconfining temperature for a non-rotating system in the infinity-volume limit.

The gauge fields can be expanded as: $A_\mu = A_\mu^{\text{cl}} + B_\mu$, $B_\mu$ is the quantum fluctuations, $A_\mu^{\text{cl}} = A_0^{\text{cl}} \delta_{\mu 0}$ .

***The 1-loop effective potential can be obtained by solving the eigenvalue problem of scalar and vector fluctuation operators in BF eff. theory.***

# Matrix model under real rotation

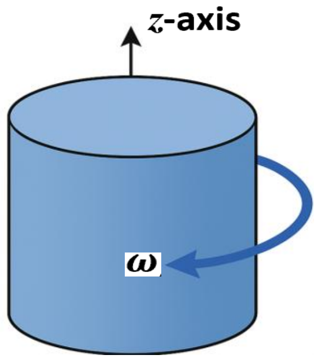


1) Confine the gluon plasma within a cylinder of radius $\boldsymbol{R}$, which **rigidly rotates** about the **fixed $z$-axis,** with $\boldsymbol{R\Omega < 1}$ to preserve the causality.

2) **Euclidean cylindrical coordinates**, laboratory reference frame: $x^\mu = (\tau, \rho, \varphi, z)$

**reference frame corotating with gluon plasma**: $\tilde{x}^\mu = (\tilde{\tau}, \tilde{\rho}, \tilde{\varphi}, \tilde{z})$

$$\tilde{\tau} = \tau\,, \quad \tilde{\varphi} = [\varphi - i\Omega\tau]_{2\pi}\,, \quad \tilde{\rho} = \rho\,, \quad \tilde{z} = z\,,$$

$[\ldots]_{2\pi}$ means modulo $2\pi$

**Only the temporal component of the covariant derivative gets modified,** $D^{\rm cl}_{\tilde{\tau}} = \partial_{\tilde{\tau}} - i\Omega\partial_{\tilde{\varphi}} - ig[A_0^{\rm cl}, \quad ]\,.$

| | Eigenvalues | Eigenmodes |
|---|---|---|
| Gluon fields | $(\tilde{E}^{ab,(1,2)}_{n\mathcal{J}})^2 = p_z^2 + \left(\frac{\kappa_{m,l}}{\mathcal{R}}\right)^2 + M^2 + (\omega_n^{ab} - im\Omega)^2\,,$<br>$(\tilde{E}^{ab,(3)}_{n\mathcal{J}})^2 = p_z^2 + \left(\frac{\kappa_{m+1,l}}{\mathcal{R}}\right)^2 + M^2 + (\omega_n^{ab} - im\Omega)^2\,,$<br>$(\tilde{E}^{ab,(4)}_{n\mathcal{J}})^2 = p_z^2 + \left(\frac{\kappa_{m-1,l}}{\mathcal{R}}\right)^2 + M^2 + (\omega_n^{ab} - im\Omega)^2\,.$<br>$\omega_n = 2\pi n T$ is the Matsubara frequency,<br>$\mathcal{J} = (m, l, p_z)$ is the cumulative index,<br>$m \in \mathbb{Z}$ is angular quantum number, | $\Psi^{(1,2)}_{n\mathcal{J}}(\tilde{\tau}, \tilde{\varphi}, \tilde{\rho}, \tilde{z}) = \Phi_{n\mathcal{J}}(\tilde{\tau}, \tilde{\varphi}, \tilde{\rho}, \tilde{z})\varsigma^{(1,2)},\quad \varsigma^{(1)} = (1,0,0,0)^T \quad \varsigma^{(2)} = (0,0,0,1)^T$<br>$\Psi^{(3)}_{n\mathcal{J}}(\tilde{\tau}, \tilde{\varphi}, \tilde{\rho}, \tilde{z}) = e^{-i\omega_n\tilde{\tau} - im\tilde{\varphi} - ip_z\tilde{z}}\frac{J_{m+1}(\frac{\tilde{\rho}}{\mathcal{R}}\kappa_{m+1,l})}{\sqrt{2\beta}\pi\mathcal{R}\lvert J_{m+2}(\kappa_{m+1,l})\rvert}\varsigma^{(3)},\quad \varsigma^{(3)} = \frac{1}{\sqrt{2}}(0,1,i,0)^T$<br>$\Psi^{(4)}_{n\mathcal{J}}(\tilde{\tau}, \tilde{\varphi}, \tilde{\rho}, \tilde{z}) = e^{-i\omega_n\tilde{\tau} - im\tilde{\varphi} - ip_z\tilde{z}}\frac{J_{m-1}(\frac{\tilde{\rho}}{\mathcal{R}}\kappa_{m-1,l})}{\sqrt{2\beta}\pi\mathcal{R}\lvert J_{m}(\kappa_{m-1,l})\rvert}\varsigma^{(4)},\quad \varsigma^{(4)} = \frac{1}{\sqrt{2}}(0,1,-i,0)^T$<br>$l \geq 1$ is the radial quantum numbers,<br>$p_z \in \mathbb{R}$ is the longitudinal quantum number,<br>$\kappa_{ml}$ is the $\ell$th positive root of the Bessel function $J_m$. |
| Ghost fields | $(\tilde{E}^{ab}_{n\mathcal{J}})^2 = p_z^2 + \left(\frac{\kappa_{m,l}}{\mathcal{R}}\right)^2 + M^2 + (\omega_n^{ab} - im\Omega)^2$ | $\Phi_{n\mathcal{J}}(\tilde{\tau}, \tilde{\rho}, \tilde{\varphi}, \tilde{z}) = e^{-i\omega_n\tilde{\tau} - im\tilde{\varphi} - ip_z\tilde{z}}\frac{J_{m}(\frac{\tilde{\rho}}{\mathcal{R}}\kappa_{m,l})}{\sqrt{2\beta}\pi\mathcal{R}\lvert J_{m+1}(\kappa_{m,l})\rvert}$ |

# Matrix model under real rotation

- Effective potential

$$\mathcal{V}(\Omega,\tilde\rho)=\frac{T}{2}\sum_{ab}\left(1-\frac{1}{N}\delta^{ab}\right)\sum_n\sum_{\mathcal{J}}\left\{\ln[\beta^2(\tilde E^{ab,(3)}_{n\mathcal{J}})^2]\boxed{\frac{J^2_{m+1}(\frac{\tilde\rho}{\mathcal{R}}\kappa_{m+1,l})}{J^2_{m+2}(\kappa_{m+1,l})}}+\ln[\beta^2(\tilde E^{ab,(4)}_{n\mathcal{J}})^2]\boxed{\frac{J^2_{m-1}(\frac{\tilde\rho}{\mathcal{R}}\kappa_{m-1,l})}{J^2_{m}(\kappa_{m-1,l})}}\right\},$$

with: $\sum_{\mathcal{J}}=\frac{1}{2\pi^2\mathcal{R}^2}\sum_{m=-\infty}^{\infty}\sum_{\ell=1}^{\infty}\int_{-\infty}^{\infty}dp_z$ .

1) The rotated gluon plasma is inhomogeneous along the radial direction.
2) When setting $\Omega=0, R\to\infty$, we analytically reproduce the result in infinity volume limit without rotation, by

$$\sum_{\ell=1}^{\infty}\to(\mathcal{R}/\pi)\int_0^{\infty}dp_\rho\ ,\ p_\rho=\kappa_{m,l}/R\ ,\ \text{and}\ J^2_{m+1}(\kappa_{m,l})\to 2/(\pi\mathcal{R}p_\rho).$$

3) The argument of the logarithm remains positive, due to the constraint of causality and $\sum_{a=1}^{N}\mathrm{q}^a=0$ .

- Matrix model under real rotation

$$\mathcal{F}(\Omega,\tilde\rho)=\frac{M^2}{2\pi^2\mathcal{R}^2}\sum_{s,l=1}^{\infty}\sum_{m=-\infty}^{\infty}\sum_{ab}\left(1-\frac{1}{N}\delta^{ab}\right)\left[K_0\left(\beta s\frac{\kappa_{m+1,l}}{\mathcal{R}}\right)-\frac{2\kappa_{m+1,l}}{s\beta M^2\mathcal{R}}K_1\left(\beta s\frac{\kappa_{m+1,l}}{\mathcal{R}}\right)\right]$$
$$\times\cos(2s\pi\mathrm{q}^{ab})\left[\cosh(s\beta m\Omega)+\cosh(s\beta(m+2)\Omega)\right]\boxed{\frac{J^2_{m+1}(\frac{\tilde\rho}{\mathcal{R}}\kappa_{m+1,l})}{J^2_{m+2}(\kappa_{m+1,l})}},$$

where $K_0(x)$ and $K_1(x)$ are modified Bessel function of the second kind.

Bulk-averaged matrix model

$$\bar{\mathcal{F}}(\Omega)=\frac{M^2}{2\pi^2\mathcal{R}^2}\sum_{s,l=1}^{\infty}\sum_{m=-\infty}^{\infty}\sum_{ab}\left(1-\frac{1}{N}\delta^{ab}\right)\left[K_0\left(\beta s\frac{\kappa_{m+1,l}}{\mathcal{R}}\right)-\frac{2\kappa_{m+1,l}}{s\beta M^2\mathcal{R}}K_1\left(\beta s\frac{\kappa_{m+1,l}}{\mathcal{R}}\right)\right]$$
$$\times\cos(2s\pi\mathrm{q}^{ab})\left[\cosh(s\beta m\Omega)+\cosh(s\beta(m+2)\Omega)\right].$$

# Deconfining phase transition under real rotation

- The deconfining phase transition of $SU(3)$ and $SU(2)$

$\boxed{\mathcal{R} = 1/T_d}$

| | The minimum of the perturbative effective potential ($M = 0$) | The minimum of the non-perturbative effective potential (only $M \neq 0$ terms) | |
|---|---|---|---|
| $SU(3)$ | q = 0, $\ell = 1$ (Plasma always stays in the deconfining phase) | q = 1/3 | $\ell = 0$ (Plasma always stays in the confining phase) |
| $SU(2)$ | | q = 1/4 | |

***The phase transition is induced by a mechanism similar to that of the non-rotating system in the infinite-volume limit.***

**Real rotation only changes the stabilities of these vacua**, which can be expressed by curvature:

$$\kappa = |\mathcal{F}''|/[1+(\mathcal{F}')^2]^{3/2}\,.$$

- Since $\kappa \sim \cosh(s\beta m\Omega)$, for a given $T$ and $\tilde{\rho}$ , the system stability **increase** with $\Omega$, which is an extension of Kenji's work.
- Since $K_1(a/T)\cosh(b/T)$ with $a > b > 0$ **increases** with $T$, perturbative vacuum becomes more stable at higher $T$.
- We numerically find that $\tilde{\rho}$ −dependence of the curvature depend on $T$: **at low $T$**, $\kappa$ **decrease** with $\tilde{\rho}$; **at high $T$**, it behaves **non-monotonically**, with an increase at small $\tilde{\rho}$.

# Deconfining phase transition under real rotation

1) $M$ is a constant: $M = \sqrt{6}\pi/3T_d$ for $SU(3)$; $M = 2\sqrt{10}\pi/9T_d$ for $SU(2)$, same as the form in the infinity volume limit.

2) $M$ depend on $\boldsymbol{\Omega}$: $\boxed{M(\Omega) = (1 + \underline{0.1/0.28|\Omega|})M}$ Yin Jiang, Phys. Lett. B 853 (2024) 138655.

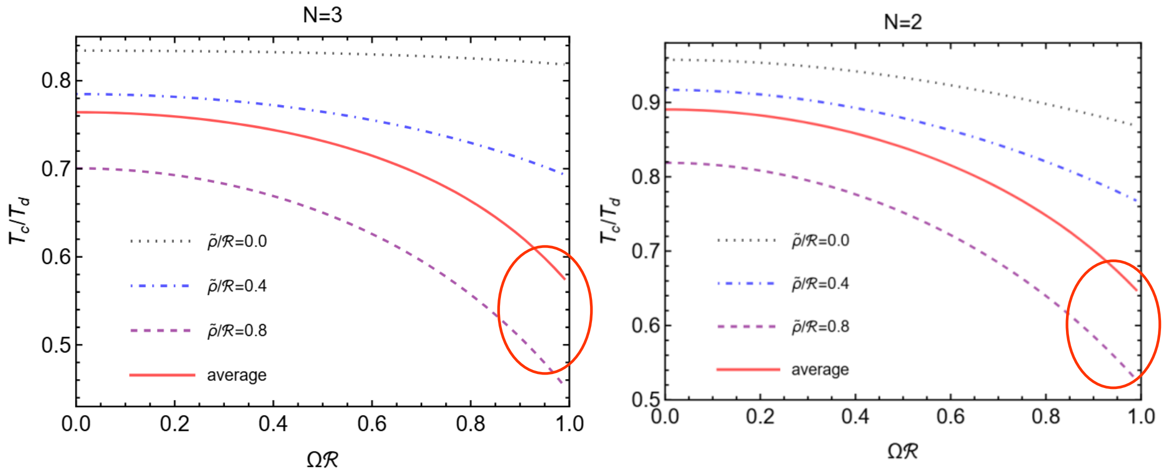


FIG. 4: $T_c/T_d$ as a function of $\Omega R$.

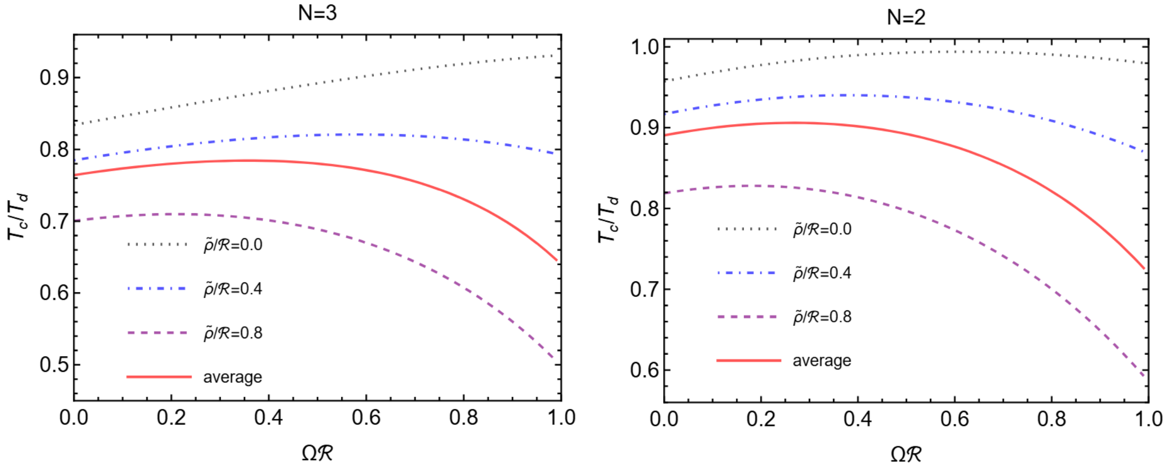


FIG. 5: $T_c/T_d$ as a function of $\Omega R$ with $M(\Omega)$.

(The solid line is the bulk-averaged result.)

**For case 1:**

- $T_c$ decreases with $\Omega$, real rotation favors deconfinment.
- The rapid decrease in $T_c$ can be understood as centrifugal effects induced by the real rotation.
- It can be perfectly described by a quadratic fit:

$$T_c(\Omega) = T_c(\Omega = 0) - g(\tilde{\rho})\Omega^2\,, \text{ with } \Omega\mathcal{R} \lesssim 0.5\,,\ g(\tilde{\rho}) > 0\,.$$

- $T_c$ at $\tilde{\rho} = 0$ is almost unaffected by rotation for $SU(3)$.

**For case 2:**

- $M(\Omega)$ qualitatively changes the behavior of $T_c$ at low $\Omega$, $T_c$ increases with small $\Omega$.
- $T_c$ exhibits a non-monotonic behavior with $\Omega$ .

***Competition between the confining effect caused by $M(\Omega)$ and rotation-induced centrifugal effect.***

# Deconfining phase transition under real rotation

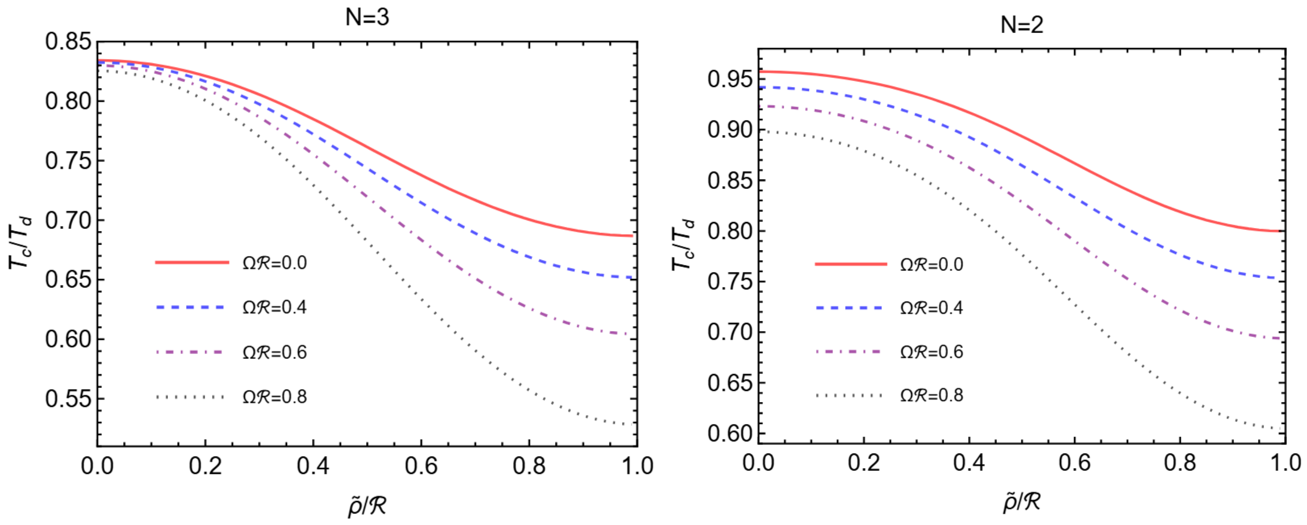


FIG. 6: $T_c/T_d$ as a function of $\tilde{\rho}/R$.

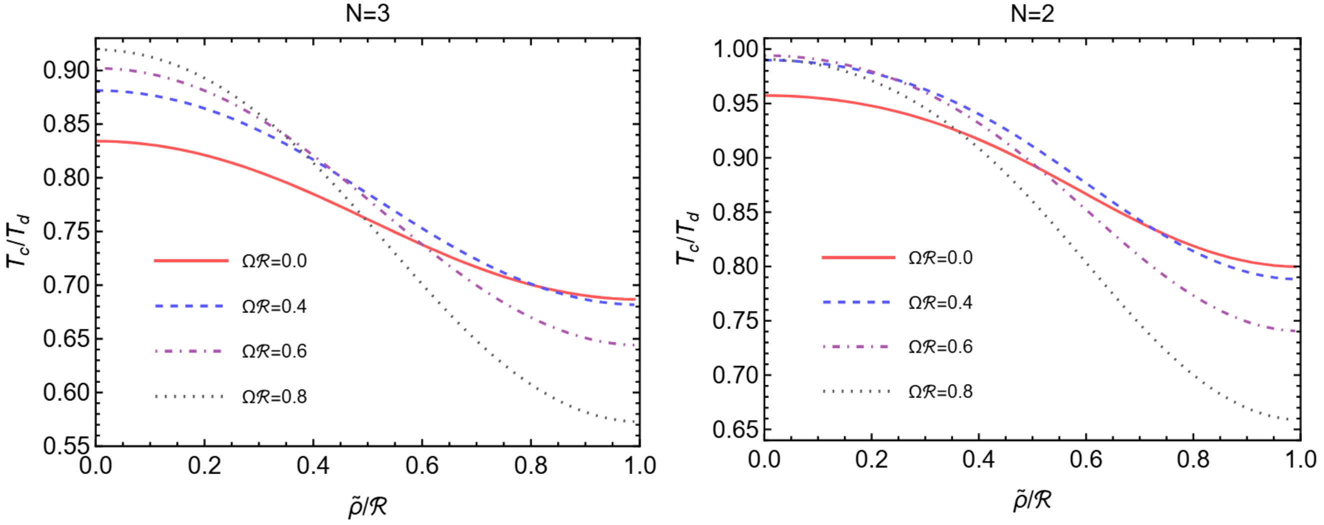


FIG. 7: $T_c/T_d$ as a function of $\tilde{\rho}/R$ with $M(\Omega)$.

- $M(\Omega)$ does not qualitatively change the behavior of $T_c$ with $\tilde{\rho}$.
- $T_c$ decreases with $\tilde{\rho}$ , which is consistent with the Tolman-Ehrenfest law.

  $T > T_c(\tilde{\rho} = 0)$: deconfined phase

  $T < T_c(\tilde{\rho} \to R)$: confined phase

  $T_c(\tilde{\rho} \to R) < T < T_c(\tilde{\rho} = 0)$:

  mixed inhomogeneous phase, with confined region at the core and a deconfined state in the outer layer.
- It can be fitted by:

  $T_c(\tilde{\rho}) = T_c(\tilde{\rho} = 0) - f(\Omega)\tilde{\rho}^2$ , with $\tilde{\rho}/\mathcal{R} \leq 0.5$ , $f(\Omega) > 0$;
- $T_c < T_d$ at $\Omega = 0$ is due to the finite-volume effect.

# Deconfining phase transition under real rotation

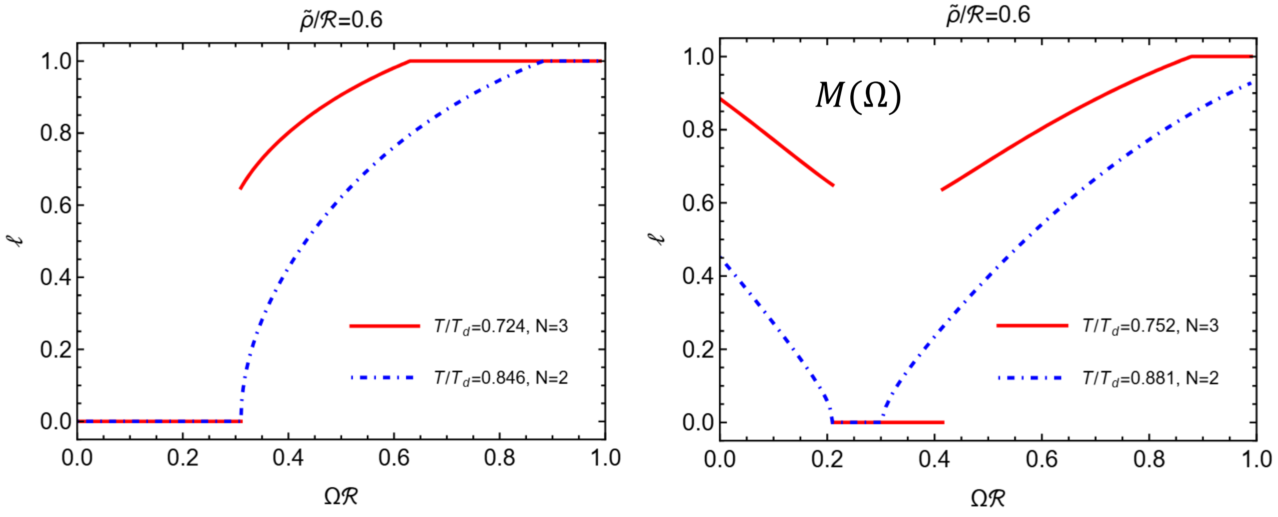


FIG. 8: $\ell$ as a function of $\Omega R$.

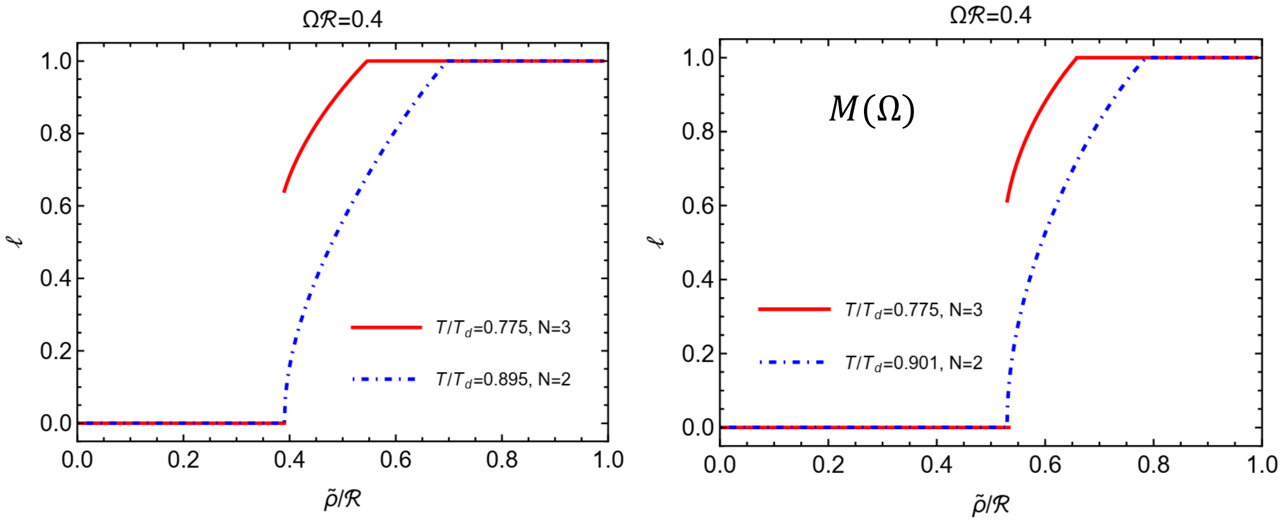


FIG. 9: $\ell$ as a function of $\tilde{\rho}/R$.

- At fixed $\Omega$ and $\tilde{\rho}$, a less reduced $T$ (relative to $T_d$) is required to drive the phase transition to deconfinement for $SU(2)$.
- For $M$ is a constant, the behavior of $\ell$ is consistent with the Tolman-Ehrenfest law, and it increase rapidly with $\Omega$ and $\tilde{\rho}$ beyond $\Omega_c$ and $\tilde{\rho}_c$.
- For $M$ depends on $\Omega$, $\ell$ becomes a non-monotonic function of $\Omega$, and there exists two $\Omega_c$.
- The nature of the phase transition is not altered by the rotation and finite-volume effect.

# Summary

- Constructed a matrix model for a rotating gluon plasma by using the background field effective theory method, and exhibited a radial inhomogeneity.
- Analytically proved the mechanism of phase transition under rotation is similar to that of the non-rotating system in the infinite-volume limit.
- Numerically investigated the behaviors of $T_c$ and $\ell$ for both $SU(3)$ and $SU(2)$.

1) $M$ is constant:

$T_c$ $(\ell)$ decrease (increase) with $\Omega$ and $\tilde{\rho}$ , and is consistent with the Tolman-Ehrenfest law.

The rotating system exhibits spatial inhomogeneity with a confined region at the core and a deconfined state in the outer layer.

2) $M$ is $\Omega$-depend, $T_c$ increase with small $\Omega$, and exhibits a non-monotonic behavior.

3) Phase transition type remains unchanged under rotation.

# Outlooks

- Incorporating the fermionic contributions in the matrix model to study the QCD phase structure and critical end point.

Thanks for your attention!